Cherenkov counting of ^{90}Sr and ^{90}Y in bark and leaf samples collected around Fukushima Daiichi Nuclear Power Plant

Takumi KUBOTA[1)]*, Yuji SHIBAHARA[1)], Satoshi FUKUTANI[1)], Toshiyuki FUJII[1)], Tomoko OHTA[2)], Munehiko KOWATARI[3)], Satoshi MIZUNO[4)], Kohichi TAKAMIYA[1)], Hajimu YAMANA[1)]

1) Research Reactor Institute, Kyoto University, Kumatori, Osaka 590-0494, Japan
2) Hokkaido University, Sapporo, Hokkaido 060-8628, Japan
3) Japan Atomic Energy Agency, Tokai, Ibaragi 319-1195, Japan
4) Nuclear Power Safety Division, Fukushima Prefectural Government, Fukushima 960-8043, Japan
*Corresponding author: t_kubota@rri.kyoto-u.ac.jp

Abstract

The radioactivity of ^{90}Sr and ^{137}Cs in environmental samples, bark and leaf, collected around the Fukushima Daiichi Nuclear Power Plant in May 2013 was determined with the aim of investigating the migration of both nuclides using their radioactivity ratio. The radioactivity of ^{90}Sr was determined by using Cherenkov counting of ^{90}Y after purification using Sr resin and that of ^{137}Cs was determined by γ-spectrometry. Quench correction in Cherenkov counting was investigated by measurements of samples spiked with purified ^{90}Y revealed that the radioactivity could be evaluated without quench correction. The radioactivity ratio of ^{90}Sr to ^{137}Cs in bark samples of 4.2×10^{-3} and 1.2×10^{-2} was compared with the results from soil samples collected in July 2011 to show that the migration of ^{90}Sr was slower than ^{137}Cs in bark and tree.

Keywords: strontium-90, cesium-137, Cherenkov counting, Fukushima nuclear accident, vegetation samples

Introduction

The accident at the Fukushima Daiichi Nuclear Power Plant led to the release of a large amount of various radioactive materials, which migrated through the atmosphere, hydrosphere, and biosphere and a part of which were chemically and physically trapped in the environment. Among the radioactive nuclides released as a result of the Fukushima accident, the environmental contamination from radioiodine and radiocesium has been well-studied previously [1-6]; these studies have reported that radioiodine spread globally while radiocesium was mainly deposited in East Japan and released into the Pacific Ocean. Radioactive strontium, not well-studied in the wake of the Fukushima accident, is still important to investigate for its migration into vegetation and accumulation in foodstuff in terms of internal exposure.

^{89}Sr and ^{90}Sr, unlike ^{137}Cs and ^{131}I, are pure beta emitter nuclides, and their radioactive measurements should be conducted after the purification of strontium from the sample matrix. Methods for purification include the use of a specific resin [7-11], solvent extraction [12], and anion exchange resin [13,14]. Radioactivity levels are then often determined using a gas flow proportional counter [7,8,11,15,16] and a liquid scintillation counter that employs scintillation fluid [10,17-21] or Cherenkov

radiation [13,14,22]. Methods that utilize Cherenkov radiation are generally more practical because the sample solution can be measured without mixing extra fluids, which prevents the recovery of the strontium fraction.

We determined the radioactivity of ^{90}Sr and ^{137}Cs in vegetation samples collected in the vicinity of the Fukushima Daiichi Nuclear Power Plant, where agricultural activities are prohibited due to high-level radioactive contamination. Thus, we collected bark and leaf samples instead of agricultural samples and investigated the migration of both nuclides in bark and tree in comparison to the radioactivity of soil samples [23]. In order to validate the Cherenkov counting for the determination of ^{90}Sr, we evaluated the extent of the quench effect by measuring and comparing the samples with and without the spike of ^{90}Y solution.

Materials and Methods

We collected vegetation samples around the Fukushima Daiichi Nuclear Power Plant from 25–28 May 2013. Bark and fresh leaves from *Cryptomeria japonica* and fresh leaves from *Artemisia indica var. maximowiczii* were collected from plants 3 km north of the power plant's Unit No. 1, and bark from *Metasequoia glyptostroboides* was collected from plants 2 km south of the unit. Air dose rates at 1 m height were measured at 1 μSv/h and 30 μSv/h from the north and south locations, respectively.

The vegetation samples were washed with distilled water under an ultrasonic wave to remove soil particles from the surface of the vegetation samples. The wet samples and the resulting suspended solution were dried at approximately 100 °C, packed in plastic bags and bottles, and stored in a desiccator before further treatment. An aliquot of each vegetation sample (2.5 g dry weight) was placed in a quartz test tube and incinerated at 600 °C in a tubular furnace. The ashed samples were then dissolved in hot concentrated nitric acid, fumed to dryness, dissolved in 0.1 M HNO_3, and centrifuged into separate supernatants. The resulting solution for each sample was treated with cation exchange resin Dowex 50WX8 (100–200 mesh), Eichrom UTEVA-resin (100–150 μm), and Eichrom Sr resin (100–150 μm) to purify the strontium fraction [24]. The strontium fraction, contained in the supernatant solution in 50 mL of 0.1 M HNO_3, was loaded into 4 mL of cation exchange resin and recovered with 20 mL of 8 M HNO_3 following a resin wash with 0.1 M HNO_3. The recovered strontium was then injected into a column filled with 1 mL of UTEVA resin to remove uranium and plutonium. The strontium fraction eluted into the first effluent was fumed to dryness and prepared to 10 mL of 3 M HNO_3 solution. This solution was injected into a column filled with 1 mL of Sr resin, resin washed with 5 mL of 3 M HNO_3, and treated with 20 mL of 0.05 M HNO_3 to recover the strontium fraction. Finally, for each sample, the radioactivity levels of ^{90}Sr and ^{90}Y in the purified strontium solution were measured by Cherenkov counting and the recovery of strontium throughout the purification was evaluated using an inductively coupled plasma quadrupole mass spectrometry (ICP-QMS, HP-4500, Yokogawa).

The Cherenkov radiation from an aliquot of the purified strontium solution (10 mL) was measured with a liquid scintillation analyzer (Tri-Carb 2700 TR, Packard), with Milli-Q water used to obtain the background value. The radioactivity of ^{137}Cs, which accounted for dominant levels of radioactivity in the samples collected around the Fukushima Daiichi Nuclear Power Plant, was measured by γ-spectrometry (a coaxial-type Ge detector, Canberra). For this measurement, energy calibration was conducted with a

certified calibration standard source (^{109}Cd, ^{57}Co, ^{139}Ce, ^{203}Hg, ^{113}Sn, ^{85}Sr, ^{137}Cs, ^{88}Y, and ^{60}Co; GE Healthcare), and solid angle correction factors were determined with potassium chloride powder and solution [25,26].

The calibration of the Cherenkov counting, the evaluation of its coefficient, and the correction of quenching in the counting were conducted using ^{134}Cs generated at the Kyoto University Research Reactor (KUR) [27] and the standard solution of ^{90}Sr was purchased from Eckert and Ziegler Isotope Products. The counting coefficients of ^{90}Sr and ^{90}Y were obtained from the increase in the radioactivity of ^{90}Y in the purified ^{90}Sr solution. The calculation is described below. The correction of quenching was conducted by the spiking of purified ^{90}Y solution to the sample strontium solution and nitric acid, as control for quenching, for comparison after quantitative analysis. The difference of the resulting increase in counting rate between both solutions showed a need to correct for quenching. Purified ^{90}Y, absent of ^{90}Sr, was spiked to avoid the spoil of sample strontium solution, whose radioactivity was finally regulated by the original ^{90}Sr after the decay of the extra radioactivity of ^{90}Y. The separation of ^{90}Sr and ^{90}Y from the standard solution was conducted by using the Sr resin method, as described above, and the radioactive purity of both fractions were 99.9%.

Calculations

We quantified levels of ^{90}Sr using the radioactivity of its daughter nuclide, ^{90}Y, which required long periods of time for measuring low-level samples. The change in ^{90}Y radioactivity during measurements must be accounted for in this process because of its relatively short half-life, and corrections for decay and growth are described in detail below. The radioactivity levels of environmental samples due to ^{90}Sr were calculated using regression analysis, with the ^{90}Y and ^{90}Sr measurement coefficient.

When radioactivity changes during measurements, the counting rate C (e.g., count per minute (CPM)) can be expressed according to the following equation:

$$C = \frac{1}{t_d}\int_{t_1}^{t_1+t_d} \sum \varepsilon_i A_i(t)dt + BG \quad (1)$$

where t_d is counting time, t_1 is the start time of counting, ε_i and A_i are the measurement coefficient and the radioactivity, respectively, of nuclide i (i.e., i = ^{90}Y, ^{90}Sr, ^{134}Cs, ^{137}Cs, ^{40}K, etc.) with the radioactivity of ^{89}Sr ignored because of its short half life causes it to decay away before the sample collection, and BG is the background value derived from the blank measurement. We used this equation for the correction of growth for ^{90}Y. The net counting rate (net CPM), Y, was then expressed according to the following equation:

$$Y = C - BG \quad (2)$$

Both measurement coefficients for ^{90}Y and ^{90}Sr were evaluated from the measurement of a standard ^{90}Sr solution in equilibrium, completely eliminated of ^{90}Y. For the measurement of the ^{90}Sr solution with the growth of ^{90}Y, Eq. (1) can be modified to the following equation:

$$Y = \frac{1}{t_d}\int_{t_1}^{t_1+t_d} \varepsilon_{\text{Y-90}} A_{\text{Y-90}}(t)dt + \varepsilon_{\text{Sr-90}} A^0_{\text{Sr-90}} \quad (3)$$

where $A^0_{\text{Sr-90}}$ is the initial radioactivity of ^{90}Sr and its decay is ignored for the short period. The

radioactivity of ^{90}Y, $A_{\text{Y-90}}(t)$, produced through the decay of ^{90}Sr, can be expressed according to the following equation:

$$A_{\text{Y-90}}(t) = \frac{\lambda_{\text{Y-90}}}{\lambda_{\text{Y-90}} - \lambda_{\text{Sr-90}}} A^0_{\text{Sr-90}} \left(e^{-\lambda_{\text{Sr-90}} t} - e^{-\lambda_{\text{Y-90}} t} \right) \quad (4)$$

where $\lambda_{\text{Y-90}}$ and $\lambda_{\text{Sr-90}}$ are the decay constants of ^{90}Y and ^{90}Sr, respectively, and the initial radioactivity of ^{90}Y is zero as ^{90}Y is eliminated by the separation of ^{90}Sr. In the short period where the decay of ^{90}Sr can be ignored, the relationship between both decay constants, $\lambda_{\text{Y-90}} >> \lambda_{\text{Sr-90}}$, simplifies the equation to the following:

$$A_{\text{Y-90}}(t) = A^0_{\text{Sr-90}} \left(1 - e^{-\lambda_{\text{Y-90}} t} \right) \quad (5)$$

This equation combined with Eq. (3), yields the following:

$$Y = \varepsilon_{\text{Sr-90}} A^0_{\text{Sr-90}} \left(1 + \alpha X \right) \quad (6)$$

where $\alpha = \frac{\varepsilon_{\text{Y-90}}}{\varepsilon_{\text{Sr-90}}}$ and $X = 1 - e^{-\lambda_{\text{Y-90}} t_1} \left(\frac{1 - e^{-\lambda_{\text{Y-90}} t_d}}{\lambda_{\text{Y-90}} t_d} \right)$, and X is the ^{90}Y saturation ratio corrected for growth during the measurement time (corrected equilibrium fraction). We conducted a regression analysis to determine the initial radioactivity of ^{90}Sr. Eq. (6) is transformed by taking the log of both sides to yield the following equation:

$$\log Y = \log \left(\varepsilon_{\text{Sr-90}} A^0_{\text{Sr-90}} \right) + \log \left(1 + \alpha X \right) \quad (7)$$

This equation is adapted to a non-linear least squares (LSQ) equation to calculate the value of α and $\log \left(\varepsilon_{\text{Sr-90}} A^0_{\text{Sr-90}} \right)$. We use only the value of α to evaluate the absolute values of both measurement coefficients in the next step, because the value of $A^0_{\text{Sr-90}}$ is not equal to the initial solution and becomes unknown through the yttrium elimination process where some of ^{90}Sr is discarded with ^{90}Y. The net CPM of the initial ^{90}Sr solution in equilibrium shows that Eq. (3) can be converted to the following:

$$Y = \varepsilon_{\text{Y-90}} A^0_{\text{Sr-90}} + \varepsilon_{\text{Sr-90}} A^0_{\text{Sr-90}} = \varepsilon_{\text{Sr-90}} \left(1 + \alpha \right) A^0_{\text{Sr-90}} \quad (8)$$

and the resulting equation provides the measurement coefficients for ^{90}Y and ^{90}Sr.

The evaluation of ^{90}Sr concentration in the environmental samples would require the consideration of coexistence of other radionuclides, even though a careful purification of strontium is conducted. In this case Eq. (1) is expressed as:

$$Y = \left(\varepsilon_{\text{Y-90}} A^0_{\text{Sr-90}} \right) X + B \quad (9)$$

where $B = \sum \varepsilon_i A_i$ with i = ^{90}Sr, ^{134}Cs, ^{137}Cs, ^{40}K, etc., and B is regarded as a constant value. After the purification of strontium, the increase in net CPM with the corrected equilibrium fraction is applied to

147 regression analysis to yield the value of $\varepsilon_{\text{Y-90}} A^0_{\text{Sr-90}}$ as the slope. Then, the value of $A^0_{\text{Sr-90}}$, the
148 concentration of ^{90}Sr in the purified solution, can be determined.
149
150 **Results and Discussion**
151 In this study, we used Cherenkov radiation generated by beta particles to detect radionuclides in
152 vegetation collected around the Fukushima Daiichi Nuclear Power Plant. Table 1 lists the characteristics
153 of major beta-emitting nuclides released from the power plant as well as those of ^{40}K, a naturally
154 occurring radionuclide with a long half-life [28]. The Cherenkov spectra of selected representative
155 radionuclides are shown in Figure 1. The width of each spectrum peak increases with increased beta
156 energy, and the spectra obtained for ^{90}Sr and ^{134}Cs were derived from similar beta energy profiles. Thus, it
157 is reasonable to suggest that the spectra of ^{137}Cs and ^{89}Sr resemble those of ^{90}Sr and ^{40}K, respectively. In
158 addition, the Cherenkov spectra obtained in this study support the purity of focal radionuclides as well as
159 the need for further purification of samples.
160 When the same amount of radioactivity is spiked to two measurement samples, the increase in
161 counting rate is expected to be the same for each unless the effect of quenching in measurement occurs.
162 We have investigated the contribution of quenching by the addition of ^{90}Y solution of 0.2 mL in 0.1 M
163 HNO_3 to the each original measurement sample where ^{90}Y was in radioactive equilibrium and in 10 mL of
164 approximately 2 M HNO_3. While this treatment changed the total volume and the resulting acid
165 concentration of the measurement samples, these changes produced no effect to the net CPM, as shown in
166 the following results. Figure 2 shows the effect of sample solution volume on net CPM where the value of
167 the net CPM is normalized to the result for the volume of 10 mL, and exhibits good agreement between
168 sample solutions of volume 5–18 mL. Figure 3 shows the effect of sample acid concentration on net CPM,
169 where the value of the net CPM is normalized to the result for the concentration of 2 M HNO_3, and
170 exhibits good agreement between HNO_3 concentrations ranging from 0.3 M to 5.4 M. These results
171 suggest that the net CPM of ^{90}Sr of 10 mL in 2 M HNO_3 will not change by addition of water or nitric
172 acid at most a few mL, which validates the spike method used to correct for quenching. Figure 4 shows
173 that the increase in the net CPM of four environmental samples spiked with ^{90}Y is normalized to the
174 standard ^{90}Sr solution spiked. The normalized value of all environmental samples is consistent among all
175 samples, which means that the measurement coefficient of the resulting solution of ^{90}Sr extracted and
176 purified from environmental samples was equal to that of standard ^{90}Sr solution. The purification of
177 strontium adequately removed impurities and quenching from the environmental samples and therefore
178 the radioactivity in the samples can be evaluated without the need for quench correction.
179 Figure 5 shows that the spectrum peak area for ^{90}Sr changed with the increase of ^{90}Y in samples
180 through time. Although the total radioactivity of the sample increased to twice the initial value at full ^{90}Y
181 saturation, the peak area was much larger than twice the initial value at full ^{90}Y saturation. This result
182 suggests the presence of different measurement coefficients between ^{90}Sr and ^{90}Y. Table 2 lists the net
183 CPM of the ^{90}Sr solution after purification to eliminate ^{90}Y. The increasing values of the net CPM with
184 increasing corrected equilibrium fraction yielded the α value of 16.7, which can be viewed in Figure 6.
185 The net CPM of 5.83 Bq ^{90}Sr in equilibrium with ^{90}Y was 208 ± 2. The values of α, net CPM, and

radioactivity of ^{90}Sr were substituted into Eq. (8) to yield measurement coefficients of ^{90}Sr and ^{90}Y of 2.01 ± 0.02 and 33.6 ± 0.3 (net CPM/Bq), respectively. These values provided the radioactivity of ^{90}Sr in the environmental samples.

Radioactivity of ^{90}Sr in the environmental samples was evaluated from aging of ^{90}Y using Eq. (9). The increase in net CPM of ^{90}Y is listed in Table 3, where the detection limit of net CPM is 5, which was evaluated with Curie's equation [29], and correspondingly 0.14 Bq from the measurement coefficient. Although both leaf samples show negligible radioactivity, both bark samples show the increase in net CPM with aging time. The increase in net CPM with aging provided the radioactivity of ^{90}Sr, which was analyzed by the regression analysis and can be viewed in Figure 7. Table 4 lists the resulting specific radioactivity of ^{90}Sr and ^{137}Cs.

The radioactivity ratio of ^{90}Sr to ^{137}Cs changing with time after the accident provides the migration tendency of both radionuclides in the environment. The radioactivity levels for all leaf samples collected from plants 3 km north of the power plant were below the detection limit. The radioactivity levels for ^{137}Cs in all samples were significant, with particularly high levels in bark samples (up to 173 Bq/g dry weight). The radioactivity ratios for the bark samples were 4.2×10^{-3} (north) and 1.2×10^{-2} (south), indicating that the fraction of ^{90}Sr to total radioactivity levels was one hundredth or less. Table 5 compares radioactivity levels of ^{90}Sr and ^{137}Cs in soil collected near the power plant before and after the nuclear accident from a previously published report [23]. The different release rates of ^{90}Sr and ^{137}Cs from the nuclear reactors caused the radioactivity of ^{137}Cs to increase to more than one hundred times to the pre-accident level while the radioactivity of ^{90}Sr increased to only several times the pre-accident level, and accordingly the radioactivity ratios decreased from 0.17 to 8.1×10^{-4} and 4.8×10^{-3}. The radioactivity of bark and soil samples collected in the vicinity of the nuclear power plants showed a larger degree of contamination in the south area and a larger isotropic release of ^{90}Sr compared to ^{137}Cs because between the north and south area there was difference in one order in radioactivity of ^{137}Cs while the order of radioactivity ^{90}Sr was the same between the north and south area. The radioactivity ratios of ^{90}Sr to ^{137}Cs in the bark samples were at least 2.4 times those of the soil samples. The radioactivity ratio in soil and bark samples would be the same value immediately after the accident due to the same contamination history at each location where the samples were collected. However, the radioactivity ratio of soil and bark samples, collected 4 months and 26 months after the accident, respectively, were different from each other, showing the different migration rate of ^{90}Sr and ^{137}Cs. The increase in the radioactivity ratio in bark samples can be ascribed to the accumulation of ^{90}Sr to bark or the diffusion of ^{137}Cs from bark. The accumulation of ^{90}Sr through root uptake is negligible because the migration rate of ^{90}Sr in soil is reported to be 0.2 – 1.0 cm/yr [30-32]. The rapid translocation of ^{137}Cs from bark into the wood was observed in Fukushima forest [33]. This increase in the radioactivity ratio in bark samples with time shows slower migration of ^{90}Sr than ^{137}Cs in bark and tree. The effect of different migration would be expected to cause considerable variation in radioactivity ratio from the initial value. The determination of ^{90}Sr in environmental samples is required to avoid suffering from unexpected '^{90}Sr hot spots.'

Conclusions

We measured the specific activity of ^{90}Sr and ^{137}Cs in leaf and bark samples collected in the vicinity of the Fukushima Daiichi Nuclear Power Plants in May 2013. The radioactivity of ^{90}Sr was quantitatively measured by using Cherenkov counting, where purified ^{90}Sr and ^{90}Y from the standard solution of ^{90}Sr were used to evaluate the measurement coefficient of Cherenkov counting and to verify the determination without any quench correction. The radioactivity of both radionuclides in the bark samples was larger than that in the leaf samples. The slower migration rate of ^{90}Sr compared to ^{137}Cs was shown by comparison to the radioactivity ratios of both radionuclides in soil samples collected in July 2011. The rough tendency of the migration in trees is shown; however, further analysis is required for the discussion of the migration of ^{90}Sr in the environment.

Acknowledgments

We wish to thank Mr. Mitsuyuki KONNO and Mr. Satoru MATSUZAKI for their help in collecting environmental samples. This work was supported by the KUR Research Program for Scientific Basis of Nuclear Safety.

References

[1] Itthipoonthanakorn T, Krisanangkura P, Udomsomporn S (2013) J Radioanal Nucl Chem 297: 419-421

[2] Povinec PP, Sykora I, Gera M, Holy K, Brest'akova L, Kovacik A (2013) J Radioanal Nucl Chem 295: 1171-1176

[3] Lee SH, Heo DH, Kang HB, Oh PJ, Lee JM, Park TS, Lee KB, Oh JS, Suh JK (2013) J Radioanal Nucl Chem 296: 727-731

[4] Tumey SJ, Guilderson TP, Brown TA, Broek T, Buesseler KO (2013) J Radioanal Nucl Chem 296: 957-962

[5] Nakanishi TM, Kobayashi NI, Tanoi K (2013) J Radioanal Nucl Chem 296: 985-989

[6] Furuta E (2013) J Radioanal Nucl Chem 297: 337-342

[7] Maxwell SL, Culligan BK, Shaw PJ (2013) J Radioanal Nucl Chem 295: 965-971

[8] Mahmood ZUW , Ariffin NAN, Ishak AK, Mohamed N, Yii MW, Ishak K, Pa'wan Z (2012) J Radioanal Nucl Chem 291: 901-906

[9] Dai X, Kramer-Tremblay S (2011) J Radioanal Nucl Chem 289: 461-466

[10] Lopes I, Madruga MJ, Mourato A, Abrantes J, Reis M (2010) J Radioanal Nucl Chem 286: 335-340

[11] Maxwell SL, Culligan BK, Shaw PJ (2010) J Radioanal Nucl Chem 286: 273-282

[12] Karacan F (2011) J Radioanal Nucl Chem 288: 685-691

[13] Grahek Z, Nodilo M (2012) J Radioanal Nucl Chem 293: 815-827

[14] Grahek Z, Karanovi G, Nodilo M (2012) J Radioanal Nucl Chem 292: 555-569

[15] Maxwell SL, Culligan BK (2009) J Radioanal Nucl Chem 279: 105-111

[16] Maxwell SL, Culligan BK (2009) J Radioanal Nucl Chem 279: 901-907

[17] Lee MH, Park TH, Park JH, Song K, Lee MS (2013) J Radioanal Nucl Chem 295: 1419-1422

[18] Solecki J, Kruk M (2011) J Radioanal Nucl Chem 289: 185-190

[19] Bhade SPD, Reddy PJ, Narayanan A , Narayan KK, Babu DAR, Sharma DN (2010) J Radioanal

Nucl Chem 284: 367-375
[20] Solecki J, Kruk M, Orzel J (2010) J Radioanal Nucl Chem 286: 27-32
[21] Dai X, Cui Y, Kramer-Tremblay S (2013) J Radioanal Nucl Chem 296: 363-368
[22] Popov L, Mihailova G, Naidenov I (2010) J Radioanal Nucl Chem 285: 223-237
[23] Fukushima prefectural government (2012)
http://wwwcms.pref.fukushima.jp/download/1/dojou120406.pdf (in Japanese)
[24] Shibahara Y, Kubota T, Fukutani S, Fujii T, Yoshikawa M, Shibata T, Ohta T, Takamiya K, Okumura R, Mizuno S, Yamana H (submitted) J Radioanal Nucl Chem
[25] Sato J, Sato K (1977) Geochemical Journal 11: 261 - 266
[26] Sato J, Hirose T, Sato K (1980) Int J App Rad Iso 31: 130-132
[27] Kubota T, Fukutani S, Ohta T, Mahara Y (2013) J Radioanal Nucl Chem 296:981-984
[28] Firestone RB, Shirley VS, Baglin CM, Chu SYF, Zipkin J (1996) The 8th edition of the Table of Isotopes, book and CD-ROM, John Wiley & Sons, Inc.
[29] Currie LA (1968) Anal Chem 40: 586-593
[30] Herranz M, Romero L.M, Idoeta R, Olondo C, Valino F, Legarda F (2011) J Environmental Radioactivity 102: 987-994
[31] Mahara Y (1993) J Env Qual 22: 722-730
[32] Fernandez J.M, Piault E, Macouillard D, Juncos C (2006) J Environmental Radioactivity 87: 209-226
[33] Kuroda K, Kagawa A, Tonosaki M (2013) J Environmental Radioactivity 122: 37-42

Tables and Figures

Table 1 Maximum energy and emission ratio of major beta-emitting radionuclides in environmental samples

Table 2 Increase in net counting rate of purified ^{90}Sr solution with the corrected equilibrium fraction of ^{90}Y (i.e., growth of ^{90}Y)

Table 3 Increase in net counting rate of purified ^{90}Sr recovered from vegetation samples with the corrected equilibrium fraction of ^{90}Y

Table 4 Radioactivity levels of ^{90}Sr and ^{137}Cs found in vegetation samples collected near the Fukushima Daiichi Nuclear Power Plant

Table 5 Radioactivity levels of ^{90}Sr and ^{137}Cs found in soil samples collected near the Fukushima Daiichi Nuclear Power Plant, as reported by [23]

Figure 1 Comparison of Cherenkov radiation spectra for ^{90}Y, ^{40}K, ^{137}Cs, and ^{90}Sr

Figure 2 Effect of sample solution volume with the same amount of ^{90}Sr on Cherenkov counting rates, normalized to the rate at 10 mL volume
SD: 2 σ

Figure 3 Effect of acid concentration on Cherenkov counting rates, normalized to the rate at the concentration of 2 M HNO_3
SD: 2 σ

Figure 4 Increase ratio in net counting rate in ^{90}Sr from vegetation samples by the spike of purified ^{90}Y in comparison to the standard ^{90}Sr solution spiked for the same amount of ^{90}Y.
SD: 2 σ

Figure 5 Change in Cherenkov spectra for purified ^{90}Sr solution with respect to the corrected equilibrium fraction of ^{90}Y.

Figure 6 Fitting line defined in Eq. (7) to evaluate the ratio of the detection coefficient of ^{90}Y and ^{90}Sr, α, using the values in Table 2

Figure 7 Regression analysis for the evaluation of radioactivity of ^{90}Sr in vegetation samples (closed circle: #1 bark *Metasequoia*; open circle: #2 bark *Cryptomeria japonica*)

329 Table 1

330

Nuclide	Maximum E_β (MeV)	Emission ratio
^{40}K	1.311	
^{89}Sr	1.495	
^{90}Sr	0.546	
^{90}Y	2.280	
^{134}Cs	0.658	70.2%
	0.415	2.5%
	0.089	27.3%
^{137}Cs	1.176	5.6%
	0.514	94.4%

331

332

333 Table 2

334

Aging Time (hr)	Counting Time (hr)	*X**	Net CPM
0.4	0.5	0.007	28.5 ± 1.5
44.4	0.5	0.383	174.0 ± 2.6
81.7	0.5	0.588	260.8 ± 3.2
123.6	0.5	0.738	323.2 ± 3.5
621.4	0.5	0.999	438.2 ± 4.0

335 **X*: Corrected Equilibrium Fraction

336

337

338 Table 3

339

#1 Bark *Metasequoia*

Aging Time (hr)	*X**	Net CPM
112.0	0.71	23.38 ± 0.98
146.7	0.80	25.00 ± 0.99
216.5	0.91	28.12 ± 1.02
289.1	0.96	29.59 ± 1.03
327.9	0.97	30.17 ± 1.03
371.4	0.98	30.08 ± 1.03

A = 25.91 ± 1.24

B = 4.73 ± 1.11

#2 Bark *Cryptomeria japonica*

Aging Time (hr)	*X**	Net CPM
131.8	0.76	6.34 ± 0.82
170.6	0.85	7.41 ± 0.83
214.1	0.90	8.34 ± 0.83
307.5	0.96	8.43 ± 0.84

A = 11.08 ± 2.13

B = -2.00 ± 1.85

#3 Leaf *Cryptomeria japonica*

Aging Time (hr)	*X**	Net CPM
136.0	0.78	1.81 ± 0.77
174.8	0.85	1.92 ± 0.77
218.3	0.91	2.02 ± 0.77
311.7	0.97	2.15 ± 0.77

#4 Leaf *Artemisia*

Aging Time (hr)	*X**	Net CPM
49.8	0.43	1.51 ± 0.76
103.8	0.68	1.46 ± 0.75
147.5	0.80	0.88 ± 0.76

340 *X**: Corrected equilibrium fraction

341 Detection limit: net CPM = 5

342

343

344 Table 4

345

Sample	Location*	^{90}Sr (Bq/g)	^{137}Cs (Bq/g)	^{90}Sr / ^{137}Cs
#1 Bark *Metasequoia*	2 km south	0.73 ± 0.04	172.9 ± 2.0	(4.2 ± 0.2) ×10^{-3}
#2 Bark *Cryptomeria japonica*	3 km north	0.31 ± 0.06	26.9 ± 0.5	(1.2 ± 0.2) ×10^{-2}
#3 Leaf *Cryptomeria japonica*	3 km north	< DL**	10.4 ± 0.2	
#4 Leaf *Artemisia*	3 km north	< DL**	4.9 ± 0.2	

346 * Location: Distance from the Fukushima Daiichi Nuclear Power Plant Unit No. 1

347 ** DL: 0.11 Bq/g

348

349

350 Table 5

351

Location*: 2 km south

Sampling Year	2005	July 2011
^{90}Sr (Bq/g)	ND**	0.0808
^{137}Cs (Bq/g)	ND**	99.7
^{90}Sr/^{137}Cs		8.1×10^{-4}

352

Location*: 3 km north

Sampling Year	2005	July 2011
^{90}Sr (Bq/g)	0.0030	0.0149
^{137}Cs (Bq/g)	0.0173	3.08
^{90}Sr/^{137}Cs	0.17	4.8×10^{-3}

353 Location*: Distance from the Fukushima Daiichi Nuclear Power Plant Unit No. 1

354 ND**: Not detected

355

356

Figure 1

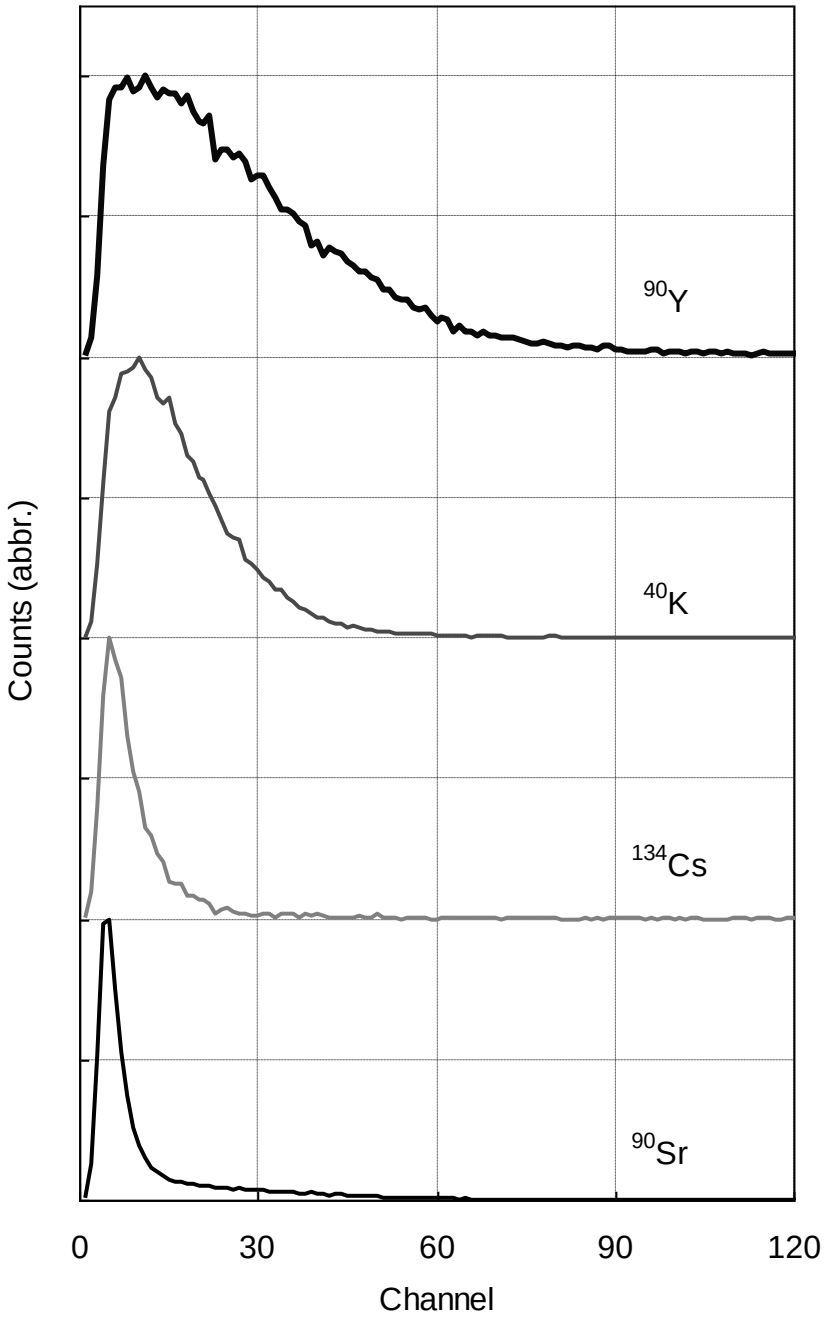

363 Figure 2

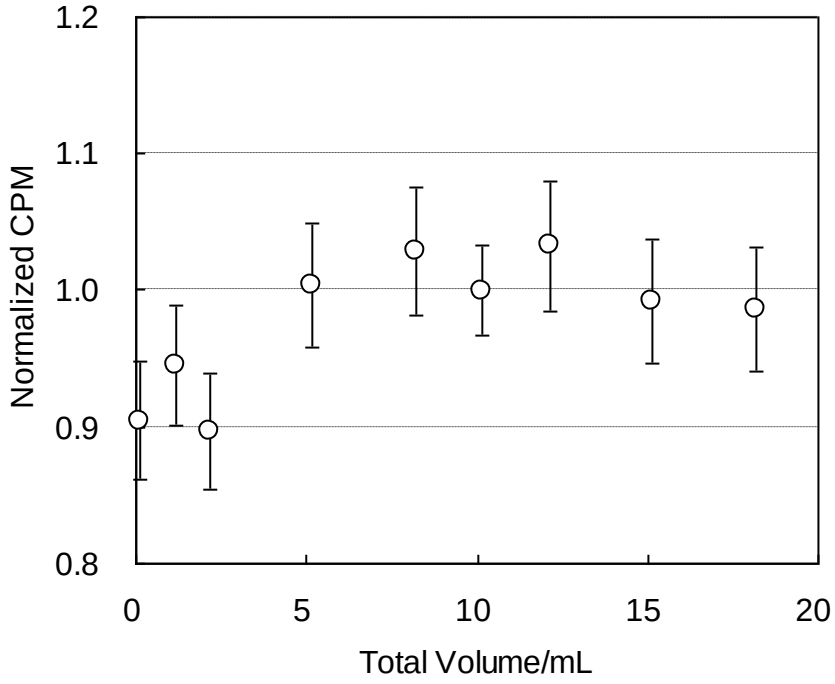

364
365
366

367 Figure 3

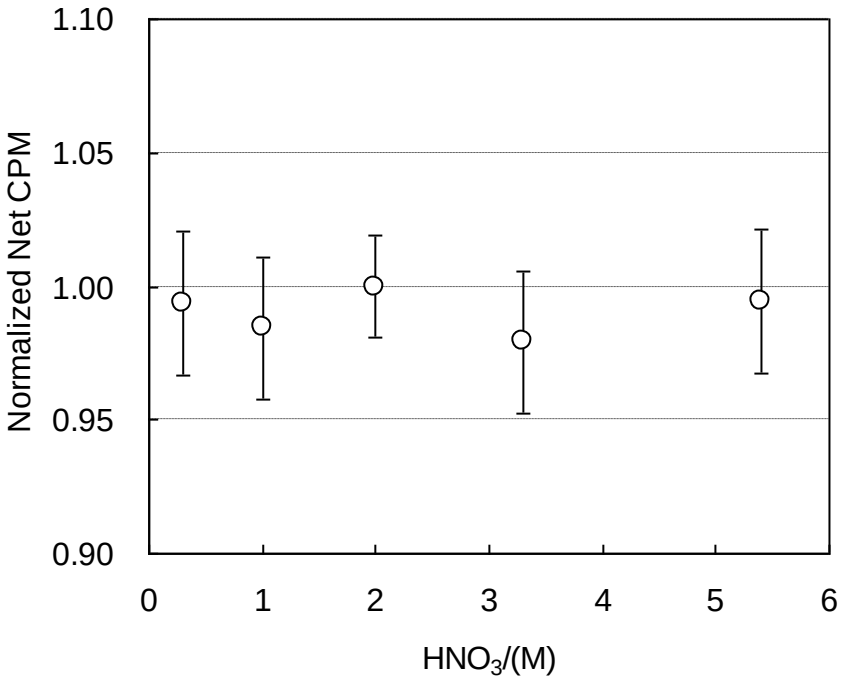

368
369
370

371 Figure 4

372

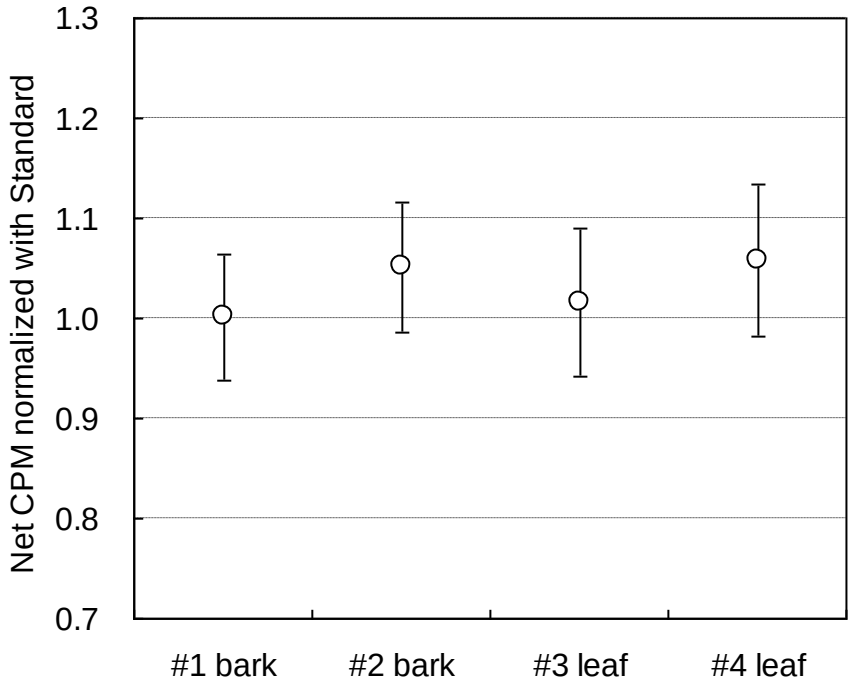

373

374

375 Figure 5

376

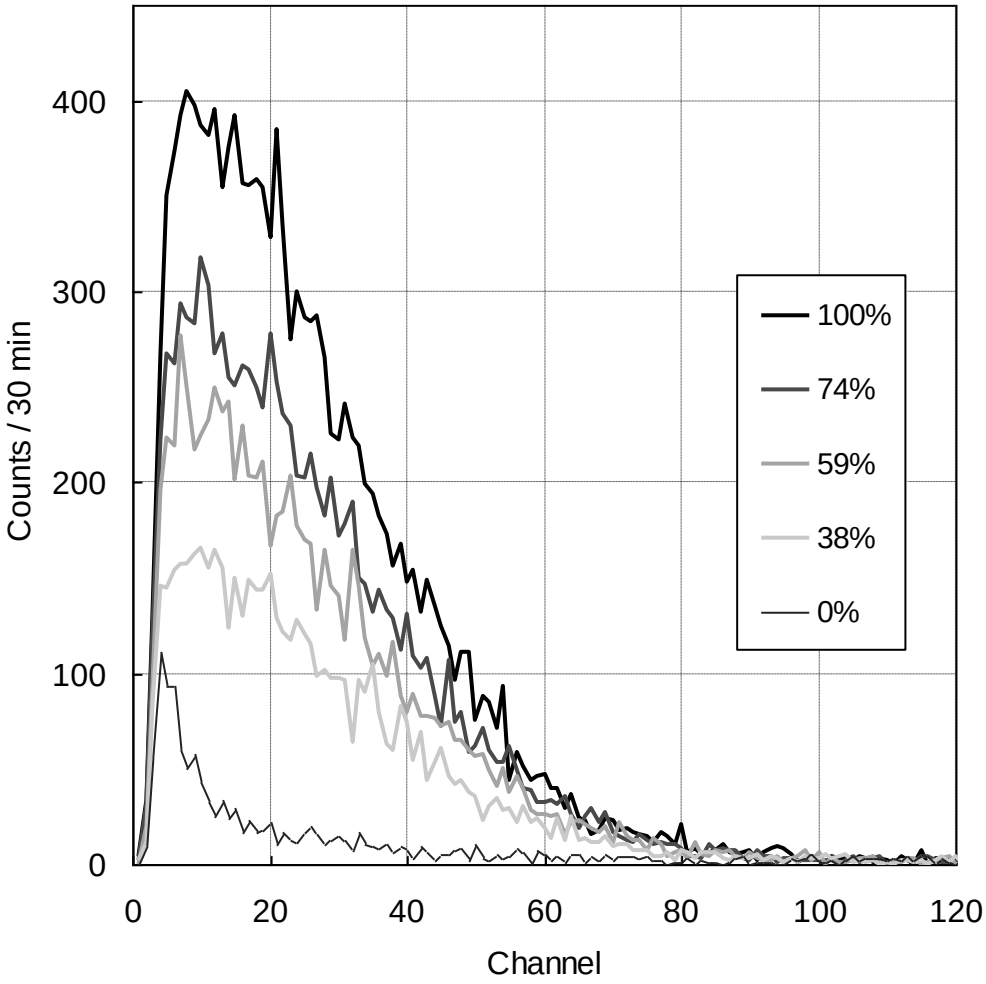

377

378

379

380 Figure 6

381

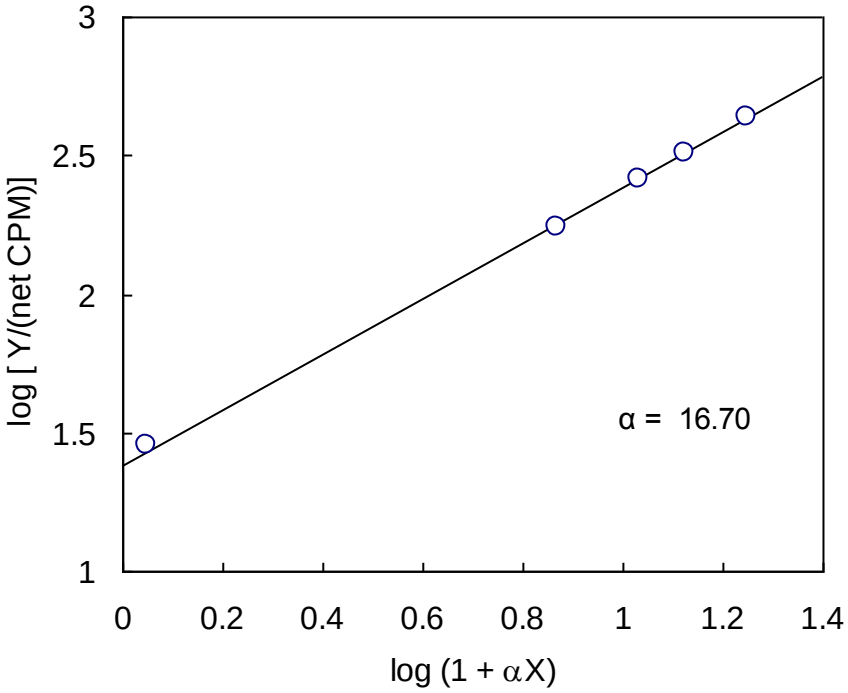

382

383

384 Figure 7

385

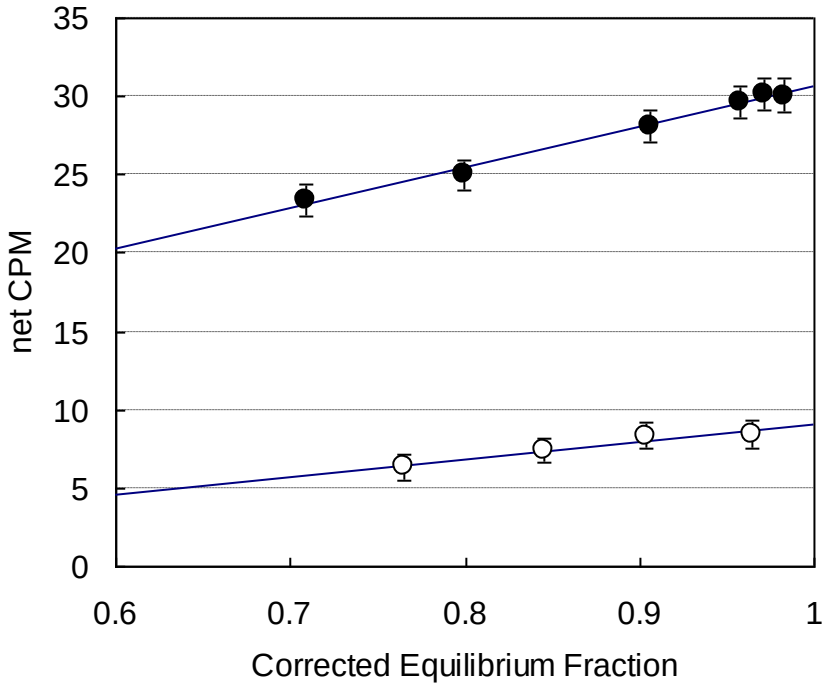

386

387